EUROPEAN LABORATORY FOR PARTICLE PHYSICS (CERN)

Search for charged Higgs Bosons in e^+e^- collisions at centre–of–mass energies from 130 to 172 GeV

The ALEPH Collaboration*)

July 21, 1997

Abstract

The data collected at centre–of–mass energies ranging from 130 to 172 GeV by ALEPH at LEP, corresponding to an integrated luminosity of 27.5 pb^{-1}, are analysed in a search for pair-produced charged Higgs Bosons $\mathrm{H}^{\pm}$. Three analyses were designed to select the $\tau^+\nu_\tau\tau^-\bar{\nu}_\tau$, $\mathrm{c\bar{s}}\tau^-\bar{\nu}_\tau$ and $\mathrm{c\bar{s}s\bar{c}}$ final states. No evidence for a signal was found. Mass limits are set as a function of the branching fraction $\mathcal{B}(\tau\nu)$ for $\mathrm{H}^{\pm} \to \tau\nu$. Charged Higgs bosons with masses below 52 GeV/c^2 are excluded at 95% C.L. independently of $\mathcal{B}(\tau\nu)$, thus significantly improving on existing mass limits from LEP1 searches.

Submitted to the 1997 lepton-photon conference, Hamburg

*) See next pages for the list of authors

1 Introduction

In the minimal Standard Model of electroweak interactions, the Higgs sector comprises only one doublet of complex scalar fields. As a result, the theory contains only one additional physical state, electrically neutral, the so-called standard Higgs boson. Despite the success of the Standard Model, no direct experimental information is available on the Higgs sector. The investigation of the implications of more complicated Higgs sectors, both in the context of the Standard Model and in extended theories, is therefore necessary.

The most important phenomenological consequence of an extended Higgs structure is the appearance of additional physical scalar states. For instance, in the simplest extensions of the minimal Standard Model (the two-doublet models), one additional doublet of complex scalar fields is introduced. Five scalar physical states remain after the spontaneous symmetry breaking mechanism has given mass to $\mathrm{W}^{\pm}$ and Z gauge bosons: three neutral bosons and a pair of charged scalar bosons. Among the possible choices, multi-doublet models are theoretically interesting because they naturally lead, at tree level, to $m_W = m_Z \cos\theta_W$ (m_W, m_Z and θ_W being, respectively, the W, Z masses and the electroweak mixing angle) and to the absence of flavour changing neutral currents, two major constraints that must be satisfied by any extension of the Standard Model to cope with the experimental observations. Another reason of interest for such models comes from the fact that one version of the two-doublet model represents the minimal Higgs sector for "low-energy" supersymmetric theories [1].

This letter describes a search for pair production of the charged Higgs bosons ($\mathrm{H}^{\pm}$) predicted in two-Higgs-doublet extensions of the Standard Model. The analysis uses the data collected by the ALEPH detector in $\mathrm{e}^+\mathrm{e}^-$ collisions delivered by LEP at centre-of-mass energies of 130, 136, 161, 170 and 172 GeV, corresponding altogether to an integrated recorded luminosity of 27.5 pb^{-1}.

In two-doublet models, charged Higgs bosons can be pair-produced through s-channel exchange of a photon or a Z boson; the couplings are completely specified in terms of the electric charge and of θ_W, making the production cross section depend only on one additional parameter, the charged Higgs boson mass m_H. The basic decay channel of the charged Higgs boson is $\mathrm{H}^+ \to \mathrm{f_u}\bar{\mathrm{f}}_\mathrm{d}$, where $\mathrm{f_u}$($\mathrm{f_d}$) is an up-type (down-type) fermion. The possibility of additional decay channels depends on the details of the models. For instance, in minimal supersymmetry several decays involving supersymmetric partners can occur. However, given the mass range addressed by this search and the present negative results of searches for supersymmetric particles, the contribution of the additional channels to the $\mathrm{H}^{\pm}$ decay width is not expected to be significant. It is therefore assumed that the $\mathrm{H}^{\pm}$ decay mostly into matter fermions. Furthermore the decay lifetime is assumed to be negligible. This is justified by the fact that in the two-doublet implementations studied so far [1], vanishing decay widths either are not possible or require a rather unnatural choice of the parameters (Higgs v.e.v.'s ratio either vanishing or very large). Although the choice for Higgs-fermion couplings is not unique [1], there is a common feature determining the phenomenology of the reaction, namely the proportionality of the coupling to fermion masses and to the relevant CKM matrix element [1]. As a consequence the predominant decays are expected to be $\mathrm{H}^+ \to \mathrm{c\bar{s}}$ or $\mathrm{H}^+ \to \tau^+\nu_\tau$ (and respective hermitian conjugated for H^-). Since the relative weight of these two main channels depends on the details of the model, no assumption is made about the decay branching fractions, and three different selections are developed to address the possible final states $\mathrm{c\bar{s}s\bar{c}}$, $\mathrm{c\bar{s}}\tau^-\bar{\nu}_\tau$ and $\tau^+\nu_\tau\tau^-\bar{\nu}_\tau$. Under the same hypothesis, the negative results of the searches performed using the first 8.5 pb^{-1} of data collected at LEP 1 allowed ALEPH to exclude charged Higgs masses lower that 41.7 GeV/c^2 at 95% CL, independently of the final state [2]. Excluded domains up to 44.1 GeV/c^2 were also reported by the other LEP experiments [3].

The letter is organised as follows. After describing the relevant parts of the ALEPH detector in Section 2, the Monte Carlo samples used for the analysis are described in Section 3. The event selections are detailed in Section 4. The results and the conclusions are given in Sections 5 and 6.

2 The ALEPH Detector

The ALEPH detector is described in detail in Ref. [4]. An account of the performance of the detector and a description of the standard analysis algorithms can be found in Ref. [5]. Here, only a brief description of the detector components and the algorithms relevant for this analysis is given.

In ALEPH, the trajectories of charged particles are measured with a silicon vertex detector, a cylindrical drift chamber, and a large time projection chamber (TPC). They are immersed in a 1.5 T axial field provided by a superconducting solenoidal coil. The electromagnetic calorimeter, placed between the TPC and the coil, is a highly segmented sampling calorimeter which is used to identify electrons and photons and to measure their energy and momentum direction. The luminosity monitors (LCAL and SICAL) extend the calorimetric coverage down to 24 mrad from the beam axis. An additional shielding against beam related background installed before the 1996 running reduces the acceptance by 10 mrad. The hadron calorimeter consists of the iron return yoke of the magnet instrumented with streamer tubes. It provides a measurement of hadronic energy and, together with the external muon chambers, muon identification.

The calorimetry and tracking information are combined in an energy flow algorithm, classifying a set of energy flow "particles" as photons, neutral hadrons and charged particles. Hereafter, charged particle tracks reconstructed with at least four hits in the TPC, and originating from within a cylinder of length 20 cm and radius 2 cm coaxial with the beam and centred at the nominal collision point, will be referred to as *good tracks*.

3 Monte Carlo Samples

The design of the selections, cut optimisation and background estimates are done using Monte Carlo event samples processed with full detector simulation, and reconstructed with the same reconstruction program used for the data. Samples of all major background sources corresponding to at least 20 times the collected luminosity have been generated. The most important background sources are $e^+e^- \to \tau^+\tau^-$, $q\bar{q}$ and four fermion processes (including WW production), simulated with KORALZ [6] and PYTHIA [7].

The signal Monte Carlo events for selection design and efficiency calculation have been generated using a version of `HZHA` [8] extended for charged Higgs boson production. The relevant features of the generator are briefly mentioned here. The initial state radiation, both for event generation and cross section calculation, is implemented by means of the `REMT` package [9], modified to account for the α^2_{QED} part of the spectrum. In the case of the hadronic decay, the hadronisation of the $c\bar{s}$ system is performed with JETSET [7]; if both H^+ and H^- decay hadronically, the resulting diquark systems are hadronised independently. In the case of $H^+ \to \tau^+\nu_\tau$, the τ polarisation is correctly transmitted to the `TAUOLA` library [10] called for the subsequent τ decay. A final state radiation treatment [11] is implemented for electrons and muons.

Samples of at least 1,000 signal events were simulated for each of the various final states for charged Higgs bosons masses varying from 40 to 70 GeV/c^2, and for each centre-of-mass energy.

4 Event selections

To ensure a good discovery potential independent of the branching fraction $\mathcal{B}(\tau\nu)$ for the decay of the Higgs into $\tau\nu$, three selections have been defined for the topologies $\tau^+\nu_\tau\tau^-\bar{\nu}_\tau$, $c\bar{s}\tau^-\bar{\nu}_\tau$ and $c\bar{s}s\bar{c}$. The most relevant selection criteria for the three selections have been chosen in order to achieve, on average and in case no signal is present, the best 95% C.L. limit on the Higgs boson production cross section [12]. The optimisation was done for each of the individual selections independently, taking the most optimistic $\mathcal{B}(\tau\nu)$ in each case, *i.e.*, 0% for the $c\bar{s}s\bar{c}$ channel, 50% for the $c\bar{s}\tau^-\bar{\nu}_\tau$ channel, and 100% for the $\tau^+\nu_\tau\tau^-\bar{\nu}_\tau$ channel. In the following sections, the three sets of selection criteria are described in detail. The performance of the analyses is summarised in Table 1 and Table 2, showing efficiencies for different Higgs boson masses and the expected background from Standard Model processes.

4.1 The $\tau^+\nu_\tau\tau^-\bar{\nu}_\tau$ final state

The final state produced by a leptonic decay of the two charged Higgs bosons consists of two acoplanar taus and missing energy carried away by the neutrinos. Since this

final state	$\tau^+\nu_\tau\tau^-\bar{\nu}_\tau$			$\mathrm{c}\bar{\mathrm{s}}\tau^-\bar{\nu}_\tau$			$\mathrm{c}\bar{\mathrm{s}}\mathrm{s}\bar{\mathrm{c}}$		
$\sqrt{s}/(\mathrm{GeV})$	133	161	172	133	161	172	133	161	172
$\epsilon(45\ \mathrm{GeV}/c^2)$	46	42	38	72	54	51	25	35	35
$\epsilon(50\ \mathrm{GeV}/c^2)$	51	45	40	71	54	50	26	38	37
$\epsilon(55\ \mathrm{GeV}/c^2)$	55	48	41	64	51	47	25	36	38
$\epsilon(60\ \mathrm{GeV}/c^2)$	58	49	43	44	42	35	22	35	38

Table 1: Efficiencies (in %) for the three analyses at the three centre-of-mass energies, given for four different Higgs masses between 45 GeV/c^2 and 60 GeV/c^2. Efficiencies in the four jet channel are quoted after all cuts, within a ± 3 GeV/c^2 window around the nominal mass.

selection	expected background			candidate events
	130, 136 GeV	161 GeV	172 GeV	130–172 GeV
$\tau^+\nu_\tau\tau^-\bar{\nu}_\tau$	1.0	0.5	1.0	1
$\mathrm{c}\bar{\mathrm{s}}\tau^-\bar{\nu}_\tau$	0.3	0.8	1.0	0
$\mathrm{c}\bar{\mathrm{s}}\mathrm{s}\bar{\mathrm{c}}$	3.1	7.9	7.7	14

Table 2: Expected number of background events from Standard Model processes for Higgs masses less than 70 GeV/c^2, in comparison with the number of events observed in the data.

topology is very similar to that defined in connection with the search for staus (the supersymmetric, scalar partner of the tau), the selections described in [13] and [14] are used here to search for charged Higgs in the $\tau^+\nu_\tau\tau^-\bar{\nu}_\tau$ channel at $\sqrt{s} = 133$ GeV and 161-172 GeV, respectively. These selections exploit the fact that the signal events contain at least four neutrinos, leading to large missing energy and a large acoplanarity of the visible system. Background from WW production followed by leptonic W decays is suppressed by vetoing events with energetic electrons or muons, which are expected to be soft when originating from τ decays.

Efficiencies to select events from $\mathrm{H}^+H^- \to \tau^+\nu_\tau\tau^-\bar{\nu}_\tau$ are of the order of 45% at $\sqrt{s} = 161$–172 GeV, as is shown in Table 1 for a representative set of Higgs boson masses. The total background expected amounts to 1.0 events at $\sqrt{s} = 130$–136 GeV and 1.5 events at $\sqrt{s} = 161$–172 GeV (see Table 2), the latter mainly consisting of irreducible background from $\mathrm{W}^+\mathrm{W}^- \to \tau^+\nu_\tau\tau^-\bar{\nu}_\tau$. In the data, one event is selected at $\sqrt{s} = 161$ GeV (see [14] for further discussion).

4.2 The $\mathrm{c}\bar{\mathrm{s}}\tau^-\bar{\nu}_\tau$ final state

The mixed final state ($\mathrm{c}\bar{\mathrm{s}}\tau^-\bar{\nu}_\tau$ or $\bar{\mathrm{c}}\mathrm{s}\tau^+\nu_\tau$) is characterised by two jets originating from the hadronic decay of one of the charged Higgs and a thin tau jet plus missing energy due to the neutrino from the decay of the other Higgs boson.

The analysis is based on two complementary approaches. In one selection, called *global* analysis, global quantities such as acoplanarity, thrust, missing momentum, are predominantly used whereas the second selection, referred to as *topological* analysis, relies more on the specific tau jet reconstruction. The analyses were designed for 161 GeV. However, only minor modifications are necessary for the data recorded at 172 GeV and 133 GeV, which will be mentioned explicitly in the description of the analyses. For the data recorded above the W pair production threshold, the inclusive combination of global and topological analysis is used. For the data recorded at 130 GeV and 136 GeV in 1995, the topological analysis is supplemented with two analyses published in [13]: the analyses for charginos for large mass differences, raising the cut on the visible mass M_{vis} to 40 GeV/c^2 and excluding the analyses with purely leptonic final states.

A preselection is common to both analyses: at least seven good tracks, whose polar angles must be greater than 18.2°, are required. The energy measured within a cone of half-angle 12° around the beam axis must be less than $2.5\%\sqrt{s}$ in order to reduce the background from tagged $\gamma\gamma$ interactions and $\mathrm{q\bar{q}}$ events with an initial state radiation photon detected at low angle. The visible mass of the event must be greater than 40 GeV/c^2 and less than 140 GeV/c^2 (172 GeV: 150 GeV/c^2, 133 GeV: 120 GeV/c^2). The quadratic mean of the inverse of the hemisphere boosts, the rejection power of which has been established in [13], is required to be greater than 0.3.

In the global analysis, to reject $\mathrm{q\bar{q}}$ events where the initial state radiation photon escapes undetected in the beam pipe, the acoplanarity angle between the two hemisphere momentum directions is required to be less than 175°. The event thrust must be less than 0.9 and the missing transverse momentum is required to amount to at least 20% of the visible energy. The missing transverse momentum direction is expected to be isolated in the signal, but not in the background. Therefore the energy contained in an azimuthal wedge of half angle 30° with respect to the missing transverse momentum direction is required to be less than $7.5\%\sqrt{s}$.

In order to reject WW events where one W decays directly to an electron or muon and a neutrino, the momentum of the leading identified lepton is required to be less than $15\%\sqrt{s}$. To deal with events where the identified lepton originates from a cascade decay via a tau, it is required that the hadronic mass of the event, *i.e.*, the visible mass excluding the leading lepton, be greater than 80 GeV/c^2. To cope with the WW background when the tau decays hadronically, the tau is identified in the following way: at least three jets must be reconstructed with the JADE algorithm using a y_{cut} of 0.001, jets with at least one and at most three tracks are considered as tau jet candidates. Ambiguities are resolved by first demanding that the total momentum carried by the charged particles of the tau jet candidates be greater than $2.5\%\sqrt{s}$ and then, if necessary, taking the jet closest to being antiparallel to the missing momentum as tau jet. This is the typical W configuration at 161 GeV where the W's are produced at rest. The other jets are merged to form the two quark jets. Since the sensitivity of this analysis is limited to charged Higgs boson masses well below the W mass, the invariant mass of the quark jets is required to be less than 70 GeV/c^2. Due to the lower Higgs boson mass, the acollinearity angle between the two jets is smaller for a Higgs boson decay than for a W decay. Therefore this acollinearity is required to be less than 130° (172 GeV: 100°).

In the topological analysis global quantities are used also, but the cuts are loosened with respect to the global analysis. The energy in the aforementioned 30° wedge is required to be less than 20%$\sqrt{s}$, the momentum of the leading lepton must be less than 20%$\sqrt{s}$, the hadronic mass is required to be less than 80 GeV/c^2 (the last cut is not applied at 133 GeV), and the missing momentum direction must point more than 25.8° away from the beam axis.

The tau jet is then identified in the Higgs configuration: at least three jets are required to be reconstructed with the JADE algorithm using a y_{cut} of 0.001. Here only jets with one charged particle track are considered as tau jet candidates and their momentum must be greater than 2.5%$\sqrt{s}$. The remaining ambiguities are resolved by choosing the jet whose angle with the missing momentum is closest to 80° as tau jet (this angle being optimal for Higgs masses in the range from 50-60 GeV/c^2). Events are rejected either if the angle between the tau jet and any other jet directions is less than 25° or if the invariant mass formed by the other jets (see Fig. 1) is greater than 60 GeV/c^2. Finally, the acollinearity angle (defined as above for the W configuration) is required to be less than 140° (172 GeV: 120°, 133 GeV: 150°).

Typical efficiencies and the background for this analysis are given in Table 1 and Table 2. The main contributions to the systematic error (3%) are the Monte Carlo statistics, the luminosity measurement (< 1%) and the requirement of the maximum energy observed within 12° of the beam pipe (< 2%), which was studied using events triggered at random beam crossings. No events were selected in the data while in total 2.1 events were expected from the Standard Model background.

4.3 The $\mathrm{c\bar{s}s\bar{c}}$ final state

For this channel, the hadronic decays of the two charged Higgs bosons lead to a final state of four well separated jets, which can be combined into two dijets with equal mass. Before exploiting the mass information, a preselection is applied to identify four jet final states.

Since the cross-sections for the two dominant background processes ($\mathrm{e^+e^-} \to \mathrm{q\bar{q}}$ and $\mathrm{e^+e^-} \to \mathrm{W^+W^-} \to \mathrm{q\bar{q}q\bar{q}}$) change considerably with the centre-of-mass energy, some of the cuts described in the following vary with $\sqrt{s}$. After requiring at least eight good tracks and a minimum charged energy of 10%$\sqrt{s}$, spherical events with thrust less than 0.9 (0.8 at $\sqrt{s}$ = 133 GeV) are clustered into four jets using the Durham algorithm. To select events with four well separated jets, a minimum Durham distance y_{34} of 0.006 (0.008) is required between all the jets. Events from $\mathrm{q\bar{q}}(\gamma)$ with an energetic initial state radiation photon undetected at small polar angles are suppressed by requiring the missing

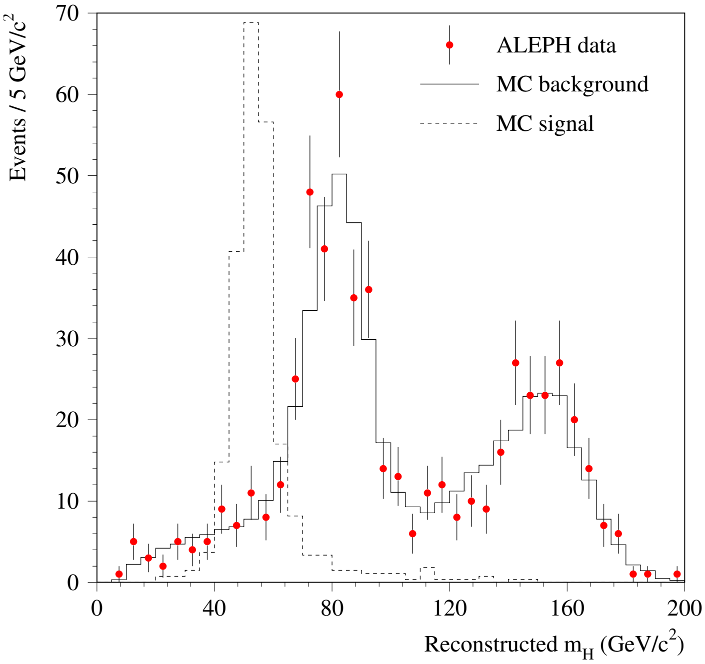

Figure 1: Distribution of the invariant mass of the quark jets, as used in the $c\bar{s}\tau^-\bar{\nu}_\tau$ selection in the Higgs configuration. The dots are the data 161 GeV and 172 GeV, the open histogram is the background expectation, normalised to the recorded luminosity. The dashed histogram is the signal for a Higgs boson mass of 55 GeV/c^2 at 161 GeV arbitrarily normalised. Only a subset of the cuts is applied to preserve sufficient statistics.

momentum $p_z^{\rm miss}$ along the beam axis to be less than $1.5 \times (M_{\rm vis} - 90)$ ($0.75 \times (M_{\rm vis} - 90)$ at $\sqrt{s} = 133$ GeV). Background with initial state radiation photons in the detector is rejected by removing events with jets that have more than 90% of its energy classified as electromagnetic energy.

At this stage charged Higgs Bosons are selected with an efficiency of about 75%. A total background of 153 events is expected, mainly consisting of events from $\rm q\bar{q}$ and $\rm W^+W^- \to q\bar{q}q\bar{q}$. The background from $\rm q\bar{q}$ can be suppressed further by requiring the jets to be compatible with coming from the decay of two particles with equal mass. As a first step, four-momentum conservation is imposed on the event to rescale the energies of the four jets, fixing the jet velocities at their measured values. After combining the jets into two dijet systems, a mass difference Δm between the two dijets is calculated for all three possible combinations. Events are selected if the minimum Δm is less than 10 GeV/c^2.

Secondly, for the events remaining, the jet momenta are determined using a five-constraint fit, imposing energy-momentum conservation and an equal mass constraint. This method leads to a dijet mass resolution of about 1.2 GeV/c^2 for a 50 GeV/c^2 Higgs at $\sqrt{s}$ =161 GeV. Events consistent with the equal mass hypothesis are selected by requiring that the χ^2 probability (see Fig. 2) be larger than 0.5 (tightened to 0.8 at 133 GeV) for the dijet combination with the best fit.

Since, given the amount of data collected so far, the sensitivity is limited to masses well below $m_{\rm W}$, most of the background from WW is not relevant for this analysis. However, in a non-negligible fraction of the WW events, a wrong jet combination gives the best fit, leading to combinatorial background at small masses. For $\sqrt{s} = 172$ GeV, this background is suppressed by vetoing events with a fitted mass m_2 (as obtained from the second best fit) close to the W mass ($|m_2 - m_{\rm W}| < 2$ GeV/c^2), applied only if the dijet mass difference Δm_2 is less than 7 GeV/c^2. Furthermore, background from both $\rm q\bar{q}$ and WW is reduced by exploiting differences in the distributions of the decay angle $\theta_{\rm dec}$ and the production angle $\theta_{\rm prod}$, summarised into a single cut $\cos\theta_{\rm prod} + 0.5\cos\theta_{\rm dec} < 1$. Here, the decay angle is defined as the angle between the dijet momentum (the 'Higgs boson' momentum) and the direction of the two jets in the Higgs boson rest frame, whereas the angle between the beam axis and the Higgs boson momentum is referred to as production angle.

After these cuts, the total background expected for reconstructed charged Higgs boson masses less than 70 GeV/c^2 amounts to 18.7 events summing over all energies (see Table 2). Efficiencies are of the order of 35% within a ± 3 GeV/c^2 mass window (see Table 1). Because of the small amount of data and the high level of background from $\rm q\bar{q}$, the selection cuts at $\sqrt{s} = 133$ GeV are tighter than at higher energy, leading to a lower efficiency at this energy. The excess of four jet events previously observed at $\sqrt{s} = 130$–136 GeV is not consistent with the equal mass hypothesis (see [15]). These events show up as an excess at small values of prob(χ^2) (see Fig. 2), and are therefore not selected by this analysis.

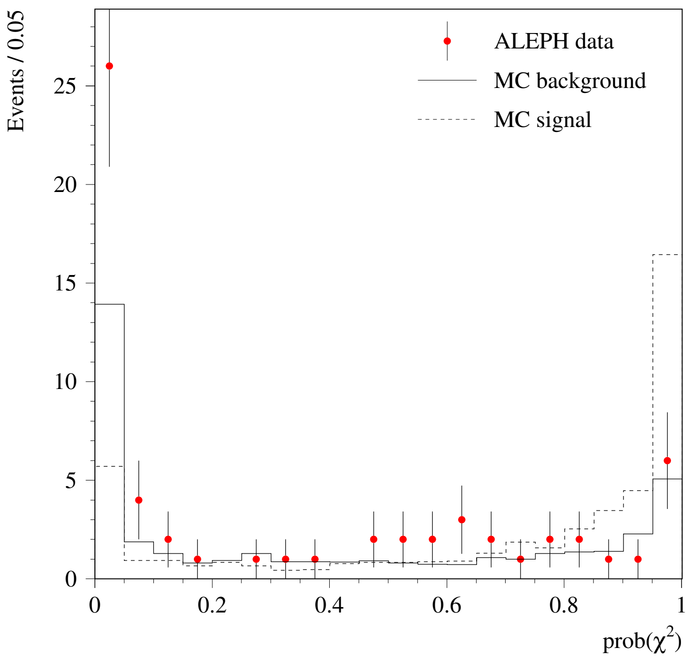

Figure 2: The χ^2 upper tail probability for the dijet combination giving the best fit, plotted for reconstructed masses less than 60 GeV/c^2 after applying the four jet preselection. The points represent the data at $\sqrt{s} = 130 - 172$ GeV. The dashed line shows the signal distribution for a Higgs boson mass of 50 GeV/c^2 in an arbitrary normalisation.

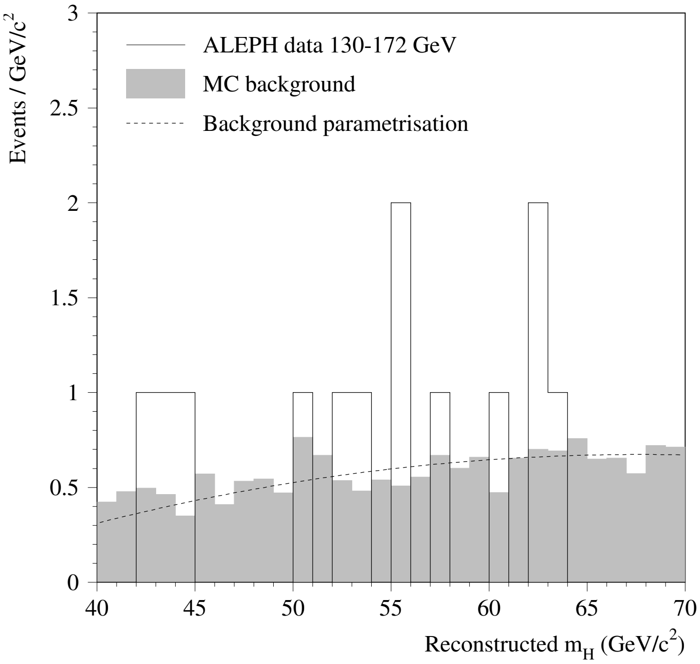

Figure 3: Distribution of the mass as obtained from the five constraint fit, applying all cuts of the $c\bar{s}s\bar{c}$ selection.

Given the relatively large amount of irreducible background, the sensitivity of the analysis is considerably increased by subtracting the expected background from Standard Model processes. For this purpose the dijet mass distribution as obtained from the background Monte Carlo has been parametrised by a polynomial. The comparison with the data (see Fig. 3) shows that both shape and normalisation of the parametrisation are compatible with the observations. In the following, this background estimate is conservatively reduced by 20%, corresponding to the statistical uncertainty of this comparison.

The systematic error on the efficiency is estimated to be 2%, dominated by the statistical uncertainty due to limited Monte Carlo statistics, with small additional contributions from the luminosity measurement and energy flow reconstruction [16].

5 Results

In the data collected at centre-of-mass energies from 130 to 172 GeV, a total of 15 events are retained by the three selections presented in Section 4 (one event in the $\tau^+\nu_\tau\tau^-\bar{\nu}_\tau$ channel, fourteen events in the $c\bar{s}s\bar{c}$ channel, and none in the mixed channel) for reconstructed charged Higgs boson masses less than 70 GeV$/c^2$, in agreement with the

23.3 events expected from Standard Model processes (see Table 2). Since, in addition, the mass distribution in the $c\bar{s}s\bar{c}$ channel does not show any significant accumulation (see Fig. 3), the result of the three selections are combined to set a 95% C.L. level limit on the charged Higgs boson mass, in the following way.

First, the confidence level is determined for each of the three selections as explained in Ref. [17], as a function of m_{H} and $\mathcal{B}(\tau\nu)$. In the $\tau^+\nu_\tau\tau^-\bar{\nu}_\tau$ and $c\bar{s}\tau^-\bar{\nu}_\tau$ channels, where no background subtraction is performed, the confidence level is conservatively defined as the fraction of outcomes of all possible experiments *with signal only* of mass m_{H} and branching fraction $\mathcal{B}(\tau\nu)$ for which the number of events selected would be smaller than or equal to the number of events observed in the actual experiment. (No mass information is included in this procedure.)

For the $c\bar{s}s\bar{c}$ channel, where background subtraction is performed, the confidence level is defined as the fraction of outcomes of all possible experiments *with signal and background* of mass m_{H} and branching fraction $\mathcal{B}(\tau\nu)$, for which the number of events selected in a mass window of ± 3 GeV/c^2 around m_{H} would be smaller than or equal to the number of events observed in this window. In order not to benefit from the fact that fewer events than expected from Standard Model processes might be observed in that window, this confidence level is renormalised to the fraction of outcomes of all possible experiments *with background only* that satisfy the same condition. This procedure was checked to always lead to a conservative estimate of the confidence level for a given signal hypothesis.

Then, the three confidence levels thus obtained are combined, for all values of m_{H} and $\mathcal{B}(\tau\nu)$ according to the democratic prescription of Ref. [17], by computing the fraction of all possible experiment outcomes that would lead to a value of the product of the three individual confidence levels smaller than or equal to the observed product. Although the analytical formulae of Ref. [17] are not valid in the case of simple event counting (generating discrete confidence level distributions), they were checked to always lead to slightly conservative results in that case, and are therefore used in the derivation of the combined confidence levels.

The result of the combination is displayed in Fig. 4, where the lines corresponding to a confidence level of 0.1%, 1%, 5% (equivalent to a 95% C.L. exclusion), 10% and 30% are drawn. Also shown are the domains excluded at 95% C.L. by the three individual analyses. It can be seen that the slight excess of events observed in the $c\bar{s}s\bar{c}$ channel around 53 GeV/c^2 (see Fig. 3) degrades the limit obtained with the $c\bar{s}\tau^-\bar{\nu}_\tau$ channel alone, for which a deficit of events was observed (0 for 2.1 expected).

6 Conclusions

A search for pair-produced charged Higgs bosons in the three channels $\tau^+\nu_\tau\tau^-\bar{\nu}_\tau$, $c\bar{s}\tau^-\bar{\nu}_\tau$ and $c\bar{s}s\bar{c}$ has been performed using 27.5 pb^{-1} of data collected at $\sqrt{s} = 130 - 172$ GeV.

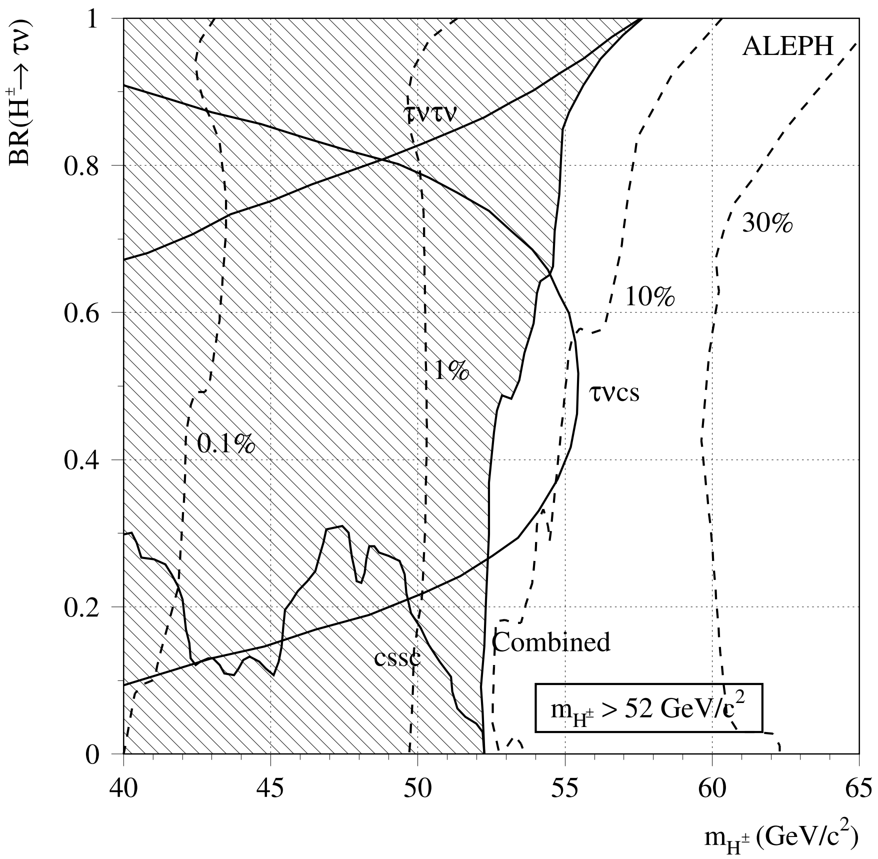

Figure 4: Limit at 95% C.L. on the mass of charged Higgs bosons as a function of $\mathcal{B}(\tau\nu)$. The three full lines show the 95% C.L. domains excluded by each of the three single analyses, whereas the hatched region marks the region excluded when combining all three channels. The dashed lines indicate various combined confidence level values.

No signs for Higgs boson production were found and mass limits were set as a function of $\mathcal{B}(\tau\nu)$. Charged Higgs bosons with masses below 52 GeV/c^2 are excluded at 95% C.L. independently of $\mathcal{B}(\tau\nu)$, improving limits previously set at LEP1.

7 Acknowledgements

It is a pleasure to congratulate our colleagues from the accelerator divisions for the successful operation of LEP above the W threshold. We would like to express our gratitude to the engineers and support people at our home institutes without whose dedicated help this work would not have been possible. Those of us from non–member states wish to thank CERN for its hospitality and support.

References

[1] J.F.Gunion, H.E.Haber, G.Kane and S.Dawson, "*The Higgs Hunter's Guide*", Frontiers in Physics, Lecture Note Series, Addison Wesley.

[2] ALEPH Collaboration, Phys. Rep. **216** (1992) 253.

[3] L3 Collaboration, Z. Phys. **C 57** (1993) 355;
OPAL Collaboration, Phys. Lett. **B 370** (1996) 174.

[4] ALEPH Collaboration, Nucl. Instr. Meth. **A 294** (1990) 121.

[5] ALEPH Collaboration, Nucl. Instr. Meth. **A 360** (1995) 481.

[6] S.Jadach and Z.Wąs, Comp. Phys. Comm. **36** (1985) 191.

[7] T.Sjöstrand, "*The PYTHIA 5.7 and JETSET 7.4 Manual*", LU-TP 95/20, CERN-TH 7112/93, Comp. Phys. Comm. **82** (1994) 74.

[8] P.Janot, "*The HZHA generator*" in "*Physics at LEP2*", Eds. G.Altarelli, T.Sjöstrand and F.Zwirner, CERN 96-01 (1996), Vol.2, p.309.

[9] F.A.Berends and R.Kleiss, "*Radiative Effects in Higgs Production at LEP*", Nucl. Phys. **178** (1981) 141.

[10] R.Decker, S.Jadach and Z.Wąs, Comp. Phys. Comm. **76** (1993) 361.

[11] E.Barberio, B.van Eijk and Z.Wąs, Comp. Phys. Comm. **79** (1994) 291.

[12] J.-F. Grivaz and F. le Diberder, "*Complementary analyses and acceptance optimization in new particle searches*", LAL preprint # 92-37 (1992).

[13] ALEPH Collaboration, Phys. Lett. **B 373** (1996) 246.

[14] ALEPH Collaboration, "*Search for sleptons in e^+e^- collisions at centre-of-mass energies of 161 GeV and 172 GeV*", CERN-PPE/97-056 (1997), submitted to Phys. Lett.

[15] ALEPH Collaboration, Z. Phys. **C 71** (1996) 179.

[16] ALEPH Collaboration, "*Search for the neutral Higgs bosons of the MSSM in e^+e^- collisions at $\sqrt{s}$ from 130 to 172 GeV*", CERN-PPE/97-071 (1997), submitted to Phys. Lett.

[17] P. Janot and F. Le Diberder, *"Combining Limits"*, CERN-PPE/97-053 (1997), submitted to Nucl. Instrum. and Methods.